This article was downloaded by: [Institute of Mechanics]
On: 31 October 2013, At: 02:37
Publisher: Taylor & Francis
Informa Ltd Registered in England and Wales Registered Number: 1072954 Registered office: Mortimer House, 37-41 Mortimer Street, London W1T 3JH, UK

Journal of Adhesion Science and Technology

Publication details, including instructions for authors and subscription information:
http://www.tandfonline.com/loi/tast20

Transitions Between Different Contact Models

Yin Zhang [a]

[a] State Key Laboratory of Nonlinear Mechanics (LNM), Institute of Mechanics, Chinese Academy of Sciences, Beijing 100080, People's Republic of China;, Email: zhangyin@lnm.imech.ac.cn

Published online: 02 Apr 2012.

To cite this article: Yin Zhang (2008) Transitions Between Different Contact Models, Journal of Adhesion Science and Technology, 22:7, 699-715

To link to this article: http://dx.doi.org/10.1163/156856108X309648

PLEASE SCROLL DOWN FOR ARTICLE

Taylor & Francis makes every effort to ensure the accuracy of all the information (the "Content") contained in the publications on our platform. However, Taylor & Francis, our agents, and our licensors make no representations or warranties whatsoever as to the accuracy, completeness, or suitability for any purpose of the Content. Any opinions and views expressed in this publication are the opinions and views of the authors, and are not the views of or endorsed by Taylor & Francis. The accuracy of the Content should not be relied upon and should be independently verified with primary sources of information. Taylor and Francis shall not be liable for any losses, actions, claims, proceedings, demands, costs, expenses, damages, and other liabilities whatsoever or howsoever caused arising directly or indirectly in connection with, in relation to or arising out of the use of the Content.

This article may be used for research, teaching, and private study purposes. Any substantial or systematic reproduction, redistribution, reselling, loan, sub-licensing, systematic supply, or distribution in any form to anyone is expressly forbidden. Terms & Conditions of access and use can be found at http://www.tandfonline.com/page/terms-and-conditions

VSP

Journal of Adhesion Science and Technology 22 (2008) 699–715

Journal of ADHESION SCIENCE and TECHNOLOGY
www.brill.nl/jast

Transitions Between Different Contact Models

Yin Zhang *

State Key Laboratory of Nonlinear Mechanics (LNM), Institute of Mechanics, Chinese Academy of Sciences, Beijing 100080, People's Republic of China

Received in final form 2 March 2008

Downloaded by [Institute of Mechanics] at 02:37 31 October 2013

Abstract

The transitions between the different contact models which include the Hertz, Bradley, Johnson–Kendall–Roberts (JKR), Derjaguin–Muller–Toporov (DMT) and Maugis–Dugdale (MD) models are revealed by analyzing their contact pressure profiles and surface interactions. Inside the contact area, surface interaction/adhesion induces tensile contact pressure around the contact edge. Outside the contact area, whether or not to consider the surface interaction has a significant influence on the contact system equilibrium. The difference in contact pressure due to the surface interaction inside the contact area and the equilibrium influenced by the surface interaction outside the contact area are physically responsible for the different results of the different models. A systematic study on the transitions between different models is shown by analyzing the contact pressure profiles and the surface interactions both inside and outside the contact area. The definitions of contact radius and the flatness of contact surfaces are also discussed.
© Koninklijke Brill NV, Leiden, 2008

Keywords

Contact, contact pressure, adhesion/surface energy, elastic deformation

Nomenclature

a, r	contact radius and polar coordinate, respectively,
D	separation gap between two spheres,
E_1, E_2	Young's moduli of two spheres,
ν_1, ν_2	Poisson ratios of two spheres,
E	effective Young's modulus and $\frac{1}{E} = \frac{1-\nu_1^2}{E_1} + \frac{1-\nu_2^2}{E_2}$,
F_{vdW}	van der Waals force outside the contact area,
h, h_0	the JKR model neck height and the height of cohesive zone, respectively,
p_{d}	Dugdale tensile stress,
p_0, p_0'	compressive and tensile contact pressures at the center, respectively,

* Tel.: +86-10-8254 3970; Fax: +86-10-8254 3977; e-mail: zhangyin@lnm.imech.ac.cn

© Koninklijke Brill NV, Leiden, 2008 DOI:10.1163/156856108X309648

p	contact pressure profile, and $p(r) = p_0(1 - r^2/a^2)^{1/2} + p_0'(1 - r^2/a^2)^{-1/2}$ in the JKR model,
P	external loading force,
$-P_c$, a_c	pull-off force and radius of the JKR model, respectively,
F, A, B	dimensionless quantities defined as $F = \frac{P}{P_c}$, $A = \frac{a}{a_c}$ and $B = \frac{r}{a_c}$,
R_1, R_2	radii of two spheres,
$R = R_1R_2/(R_1 + R_2)$,	
u_1, u_2	elastic deformations of two contacting bodies,
u_B, u_H	elastic deformations due to the Boussinesq pressure and the Hertz pressure, respectively,
$W = W(D)$	surface interaction energy of two spheres with a separation gap of D,
z_0, $-\sigma_0$	equilibrium separation of atoms and theoretical stress of the material, respectively,
δ	mutual approach of two spheres,
γ	surface energy per unit area of a surface,
κ	dimensionless parameter defined as $\kappa = W(D)/(2\gamma)$,
μ, λ	Tabor number and elastic parameter, respectively, $\mu = [R\gamma^2/(E^2z_0^3)]^{1/3}$ and $\lambda = 1.16\mu$.

1. Introduction

Hertz [1] and Boussinesq [2] independently worked out the famous contact theory known as the Hertzian theory [3]. The Hertzian theory does not incorporate the surface interaction known as the adhesion effect. The pull-off force in the Hertz model is zero. If considering the surface interaction, Bradley [4] found that the amount of external force required to pull off two rigid spheres was $-4\pi\gamma R$ (in this paper, negative value of force/pressure indicates tensile force/pressure and positive value denotes compressive ones). Derjaguin [5] gave a more general calculation form for the pull-off force of two spheres separated with a varying distance D by using an approximation known as the Derjaguin approximation [6]. The Derjaguin pull-off force is $-2\pi RW(D)$ and $W(z_0) = 2\gamma$. Therefore, Derjaguin's pull-off force corresponds to Bradley's [4]. Johnson, Kendall and Roberts [7] developed their famous adhesion contact model known as the JKR model. By assuming a different contact pressure profile from the Hertzian and accounting for the contribution of surface energy to the total energy of the system, the following JKR equation is obtained [7, 8]

$$\left(P - \frac{4Ea^3}{3R}\right)^2 = 16\pi\gamma Ea^3. \tag{1}$$

It is noticed that γ defined in the paper [7] and the book [8] has the difference of a factor of 2. γ defined in [7] is the surface energy per unit area of the two contacting surfaces; γ defined in [8] is the surface energy per unit area of a contacting surface.

Downloaded by [Institute of Mechanics] at 02:37 31 October 2013

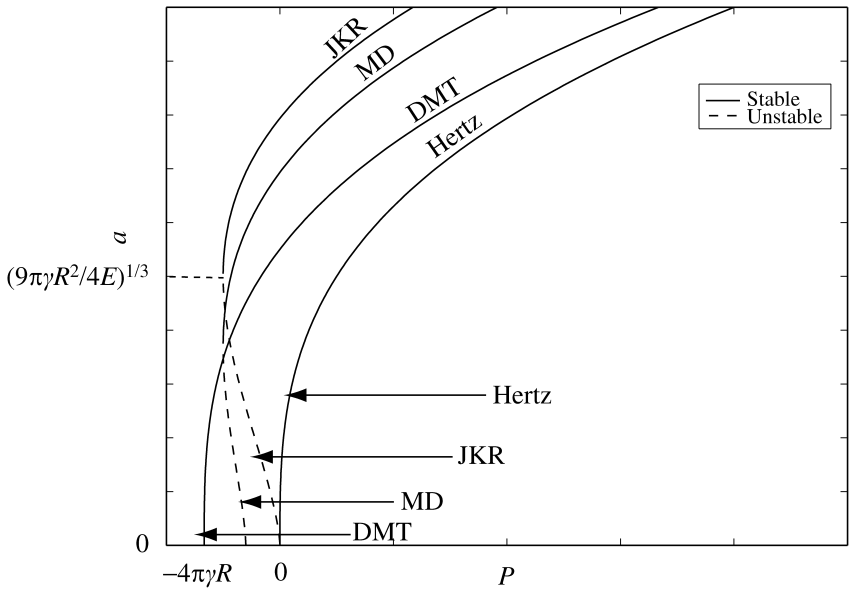

Figure 1. The P–a curves predicted by different contact models.

γ in this paper adopts the definition of the book [8]. If γ in equation (1) is set to be zero, the Hertz equation ($P = 4Ea^3/3R$) is obtained. The JKR model of equation (1) predicts a larger contact radius/area than that by the Hertzian model (see Fig. 1) under the same load P because of the adhesion effect. Derjaguin, Muller and Toporov [9] developed a model known as the DMT model. Heated debates on the JKR and DMT models were exchanged for years in the *Journal of Colloid and Interface Science* [10–13]. The P–a curves from different contact models are presented in Fig. 1. Besides the difference in the P–a curves, a significant (physical) difference of the JKR model from the Hertz and DMT models is that the Hertz and DMT models predict that the two contacting elastic bodies follow a continuous and stable path until the separation at $a = 0$; the JKR model predicts that at an unstable point with $-P_c = -3\pi\gamma R$ and $a_c = (9\pi\gamma R^2/4E)^{1/3}$, the two elastic bodies will have a sudden jumping separation [7, 8].

Maugis [3] used Dugdale's approximation [14] for the Lennard-Jones potential and a fracture mechanics approach to develop a model known as the Maugis–Dugdale (MD) model. The MD model introduces a dimensionless transition number called elastic parameter (λ) to show the transition between the DMT and JKR models. The elastic parameter is related to the Tabor number as $\lambda = 1.16\mu$ [15, 16]. Maugis [3] shows that as $\lambda \to 0$, the MD model approaches the DMT model and as $\lambda \to +\infty$, the MD model approaches the JKR model. Johnson and Greenwood [16] constructed their famous 'adhesion map' using two-dimensionless parameters $\bar{P} = P/(2\pi\gamma R)$ and λ (or μ) as the coordinates. The demarcations of the different models in the adhesion map are the curves of two ratios, i.e., the ratio

Downloaded by [Institute of Mechanics] at 02:37 31 October 2013

of the adhesion force to the total force P and the ratio of σ_a/h_0 (σ_a is the elastic deformation due to adhesion forces and $h_0 = 0.97z_0$) [16].

Realizing the difference in different contact models, Maugis [3], Johnson and Greenwood [16], Kim *et al.* [17] used different approaches to analyze and show the transitions of some of the above models. Here we present a more comprehensive transition study by analyzing the contact pressure profiles and the surface interactions both inside and outside the contact area, which affect the contact pressure as well as equilibrium. The assumptions of some contact models are also analyzed and by analyzing them, the applicability range of different contact models is also evaluated. Through the analysis of the contact pressure profiles and surface interactions, the transitions of different contact models are systematically demonstrated. As shown later in this paper, the contact area of the Hertz and JKR models is proved to be flat. This flatness of contact area is an important assumption in the 'hard' contact models, which is also the main reason causing the difference between the 'hard' and 'soft' contact models. We also find that in different contact models, the physical meanings/definitions of contact radius are different. Therefore, besides the physical reasons (i.e., the contact pressure profiles and surface interactions), the different definitions of contact radius also contribute to the differences of different contact models. Unlike the adhesion map of Johnson and Greenwood [16] which uses the two ratios mentioned above to demarcate the applicability zones of the different contact models, this paper offers a direct approach to illustrate both mathematically and physically how exactly these different contact models transit to one another.

2. Surface Interactions Inside the Contact Area: Contact Pressure Analysis

2.1. Transition Between the JKR and Hertz Models

The contact pressure profile in the JKR model is assumed to have the following form

$$p(r) = p_0(1 - r^2/a^2)^{1/2} + p_0'(1 - r^2/a^2)^{-1/2}, \tag{2}$$

where p_0 is the positive compressive pressure and $p_0(1 - r^2/a^2)^{1/2}$ is often called the Hertz pressure [8]. Singularity in $p(r)$ at $r = a$ is noticed. Finding p_0 is a Boussinesq problem and the detailed procedure can be found in Johnson's book [8]. p_0 has the following form

$$p_0 = \frac{2Ea}{\pi R}. \tag{3}$$

To find the negative tensile pressure p_0', Griffith's concept of energy release rate [18] in fracture mechanics needs to be introduced here. The energy release rate is defined as $G = \partial U_E/\partial S$, which has the unit of N/m. U_E is elastic energy and S is crack area. Griffith's criterion for rupture is defined as follows: if $G > G_c$, rupture is developed (in this particular contact problem, rupture means that the contact radius shrinks); if $G < G_c$, no rupture occurs and $G = G_c$ is the critical state. G_c here is a critical value and for brittle materials like glass, Griffith shows $G_c = 2\gamma$.

Downloaded by [Institute of Mechanics] at 02:37 31 October 2013

The elastic energy due to deformation is given as [8]

$$U_{\mathrm{E}} = \frac{\pi^2 a^3}{E}\left(\frac{2}{15}p_0^2 + \frac{2}{3}p_0 p_0' + p_0'^2\right). \tag{4}$$

And p_0 and p_0' also have the following relation [8]

$$\delta = \frac{\pi a}{2E}(p_0 + p_0'). \tag{5}$$

From equations (3) and (5), p_0' is found to be

$$p_0' = \frac{E}{\pi}\left(\frac{\delta}{a} - \frac{a}{R}\right). \tag{6}$$

Substituting equations (3) and (6) into equation (4), the elastic energy U_{E} now is

$$U_{\mathrm{E}} = E\left(\frac{a^5}{5R^2} - \frac{2}{3}\frac{\delta a^3}{R} + a\delta^2\right). \tag{7}$$

For a fixed δ, $\partial U_{\mathrm{E}}/\partial a$ becomes

$$\frac{\partial U_{\mathrm{E}}}{\partial a} = Ea^2\left(\frac{a}{R} - \frac{\delta}{a}\right)^2 = \frac{\pi^2 a^2}{E}p_0'^2. \tag{8}$$

The surface energy of contact area defined by the JKR model [7, 8] is $U_{\mathrm{S}} = -2\gamma\pi a^2$. For equilibrium, $\partial(U_{\mathrm{E}} + U_{\mathrm{S}})/\partial a$ vanishes, leading to

$$\frac{\pi^2 a^2}{E}p_0'^2 = -\frac{\partial U_{\mathrm{S}}}{\partial a} = 4\pi\gamma a, \tag{9}$$

i.e.,

$$p_0' = -\sqrt{\frac{4E\gamma}{\pi a}}. \tag{10}$$

The minus sign is chosen to let p_0' be tensile. Clearly the tensile contact pressure p_0' is directly determined by the surface interaction inside the contact area.

The following amount of external loading force P is required to balance the force due to elastic deformation

$$P = \int_0^a 2\pi r p(r)\,\mathrm{d}r = \left(\frac{2}{3}p_0 + 2p_0'\right)\pi a^2. \tag{11}$$

Equation (11) is the equation of equilibrium and it does not consider the surface interaction outside the contact area, which as analyzed later can be problematic in the DMT contact scenario. From equations (3), (10) and (11), the JKR P–a relation of equation (1) is obtained. The following two-dimensionless quantities are introduced

$$F = \frac{P}{P_{\mathrm{c}}}, \qquad A = \frac{a}{a_{\mathrm{c}}}, \tag{12}$$

Downloaded by [Institute of Mechanics] at 02:37 31 October 2013

where $P_c = 3\pi\gamma R$ and $a_c = (9\pi\gamma R^2/4E)^{1/3}$. $-P_c$ and a_c are the pull-off force and radius, respectively, in the JKR model when the external loading force P is the control parameter [8]. The dimensionless form of equation (1) now is as follows

$$(F - A^3)^2 = 4A^3. \tag{13}$$

Where p_0' is zero in the Hertz model. Correspondingly, equation (11) becomes $P = \frac{2}{3}p_0\pi a^2$ and equation (13) becomes $F = A^3$.

2.2. *Characteristics of Contact Pressure Profiles in the Hertz, JKR and MD Models*

With the substitution of $p_0 = 2Ea/(\pi R)$ and $p_0' = -\sqrt{4E\gamma/(\pi a)}$ in the JKR model into equation (2), the dimensionless contact pressure profile is obtained as follows

$$\sigma(B) = A\left(1 - \frac{B^2}{A^2}\right)^{1/2} - \frac{2}{3}A^{-1/2}\left(1 - \frac{B^2}{A^2}\right)^{-1/2}. \tag{14}$$

Where $\sigma(B) = p/[18E^2\gamma/(\pi^2 R)]^{1/3}$ and $B = r/a_c$. The first part $A(1 - \frac{B^2}{A^2})^{1/2}$ in the above equation is the Hertz pressure. Figure 2 compares the Hertz and JKR contact pressure profiles when the contact radius is small and large. Clearly when the contact radius is small, their difference is very significant. The difference di-

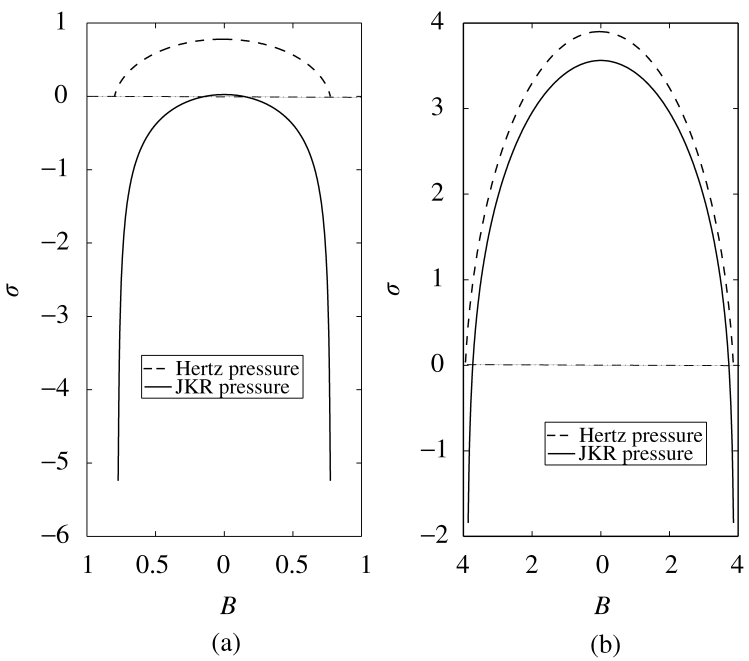

Figure 2. (a) The JKR and Hertz contact pressure profiles when A is small ($A = 0.78$). (b) The JKR and Hertz contact pressure profiles when A is large ($A = 4$).

Downloaded by [Institute of Mechanics] at 02:37 31 October 2013

minishes with the increase of the contact radius. Here it is of an interest to discuss the disappearance of the tensile contact pressure in the JKR model.

r_0 is introduced and defined as $p(r_0) = 0$. Physically, r_0 is the demarcation point of the tensile and compressive pressure zones. From equation (2), r_0 is found to be

$$r_0 = a\sqrt{1 + p_0'/p_0}, \tag{15}$$

$p(r)$ is compressive when $0 \leqslant r < r_0$ and $p(r)$ is tensile when $a \geqslant r > r_0$. For the JKR model, substituting $p_0 = 2Ea/(\pi R)$ and $p_0' = -\sqrt{4E\gamma/(\pi a)}$ in equation (15) and non-dimensionalizing it, the following dimensionless form of equation (15) is obtained

$$R_0 = A\sqrt{1 - \frac{2}{3}A^{-3/2}}. \tag{16}$$

Where $R_0 = r_0/a_c$. For R_0 to be real, the quantity inside the square root must be non-negative; therefore,

$$A \geqslant (3/2)^{-2/3}. \tag{17}$$

We define $A_{\min} = (3/2)^{-2/3} \approx 0.763$. Because the tensile contact pressure zone is $a \geqslant r > r_0$ (or $A \geqslant B > R_0$) and R_0 does not exist in real domain when $A < A_{\min}$, we can only conclude that there is *no* tensile contact pressure zone in the contact area when $A < A_{\min}$. So the JKR model itself predicts that when the contact radius reaches a critical value, there will be no tensile contact pressure zone. This was discussed by Muller, Yushchenko and Derjaguin [19] as a possibility without a detailed discussion.

Now let us examine how the JKR and DMT P–a curves are related by this disappearance of tensile contact pressure. In Fig. 1 there is an intersection point in the JKR and DMT P–a curves. Figure 3 plots the dimensionless F–A curves and the points in Fig. 3 are indicated by their corresponding F and A. For example, point $S_1 = S_1(-1, 1)$ is the critical point at which the JKR model loses the stability when P (F) is the control parameter. As mentioned before when the instability occurs, the contacting bodies will experience a displacement jump to separate from each other. At $A = A_{\min} = 0.763$, the corresponding F predicted by the JKR model is -0.89. It is also interesting to notice that $U_1(-0.89, 0.763)$ is the intersection point in the JKR and DMT F–A curves. As shown later there is no tensile contact pressure in the DMT model because it assumes the Hertzian contact pressure. It should also be pointed out that the JKR curve plotted in Fig. 3 is based on equation (13) and as analyzed above the $4A^3$ term is due to the tensile contact pressure. In Fig. 3, A continuously reduces to zero, so does $4A^3$. But we also show that the tensile contact pressure cannot exist when $A < A_{\min}$. Therefore, there is some inconsistency here. For the JKR model the stability is lost at $S_1 = S_1(-1, 1)$ when P is the control parameter, and the disappearance of tensile contact pressure does not have any influence because $A_{\min}$ is smaller than unity, so equation (13) is valid. However, it should be kept in mind that when δ is the control parameter, the JKR model loses stability at $U_2(-5/9, 0.481)$ [3, 8], which has a smaller contact radius than $A_{\min}$.

Downloaded by [Institute of Mechanics] at 02:37 31 October 2013

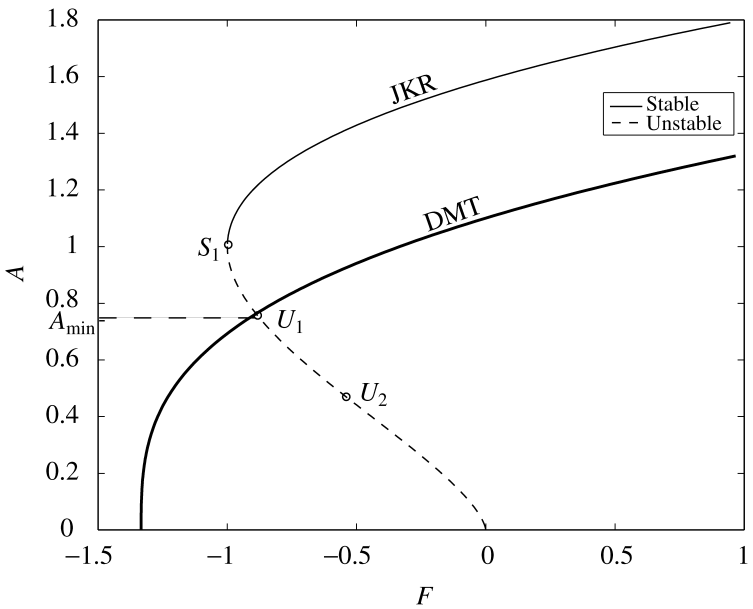

Figure 3. The F–A curves of the JKR and DMT models. The JKR curve loses stability at $S_1(-1, 1)$ when external loading force P (F) is the control parameter. $U_1(-0.89, 0.763)$ is the point below which in the JKR model the tensile contact pressure can no longer exist and it is also the intersection of the JKR and DMT curves. $U_2(-5/9, 0.481)$ is the instability point when δ is the control parameter.

The JKR contact pressure profile is derived from the Boussinesq solution of an elastic half-space, which goes to infinity at the contact edge. In the MD model there is an area called cohesive zone, in which the contact pressure is the theoretical stress of the material. Originally, the stress used by Dugdale in the cohesive zone was the yield stress [14]. Figure 4 gives schematic definition of the theoretical stress of the material ($-\sigma_0$), the cohesive zone and the MD contact pressure profiles. In Fig. 4(a), $-\sigma_0$ is the theoretical stress of the material, which is also the maximum value of the attractive force [20]. The cohesive zone is defined as $z_0 \leqslant z \leqslant z_0 + h_0$. Because $\sigma_0 h_0 = \gamma$ [16] and $\sigma_0 = 1.03\gamma/z_0$ [3, 20], $h_0 = 0.97 z_0$. The contact pressure in the MD model is as follows

$$p(r) = p_0(1 - r^2/a^2)^{1/2} + p_{\mathrm{d}}(r). \tag{18}$$

The first term is still the Hertzian pressure. p_{d} is the tensile Dugdale stress defined as follows [16]

$$p_{\mathrm{d}}(r) = \begin{cases} -\dfrac{\sigma_0}{\pi}\cos^{-1}\left(\dfrac{2a^2 - c^2 - r^2}{c^2 - r^2}\right), & r \leqslant a, \\ -\sigma_0, & a \leqslant r \leqslant c. \end{cases} \tag{19}$$

In the annulus $a \leqslant r \leqslant c$ of Fig. 4(b), the surfaces of two contacting bodies separate gradually from z_0 to $z_0 + h_0$, which is the cohesive zone. Obviously, the pressure profile from the Dugdale approximation is different from that of the JKR model.

Downloaded by [Institute of Mechanics] at 02:37 31 October 2013

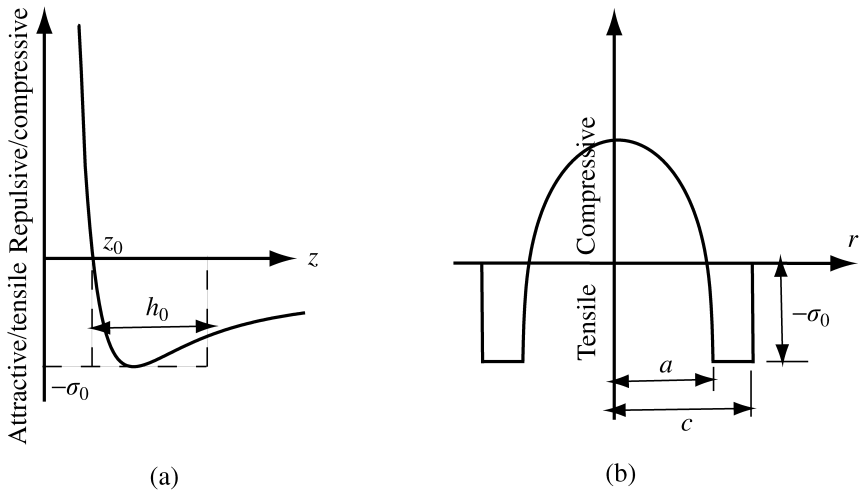

Figure 4. (a) The surface force due to Lennard-Jones potential *versus* distance z and the definitions of σ_0 and h_0. (b) Contact pressure in the MD model as a function of r.

However, a systematic numerical study by Barthel [21] shows that the solution is insensitive to the nature of surface interaction and the MD model with Dugdale approximation for surface interaction is acceptable for most contact problems.

One issue about the JKR model is that the pull-off force of $-3\pi\gamma R$ predicted by the JKR model is independent of the Young's moduli of elastic spheres as compared to $-4\pi\gamma R$ in the Bradley model for rigid spheres. As the JKR model applies to large compliant spheres (i.e., large λ or μ) [16], this pull-off force independence on Young's moduli is 'puzzling' and 'irreconcilable' with the Bradley model of rigid spheres [3]. This puzzle is solved by Maugis [3]. As λ varies from 0 to $+\infty$, the pull-off force in the MD model varies from $-3\pi\gamma R$ in the JKR model to $-4\pi\gamma R$ in the DMT model. The pull-off force in the MD model is the function of λ and $\lambda = 1.16\mu = 1.16 \times (\gamma^2 R/E^2 z_0^3)^{1/3}$. Therefore, the MD pull-off force is dependent on the Young's moduli of deformable spheres. The MD pull-off force is bounded between $-4\pi\gamma R$ and $-3\pi\gamma R$ and it monotonously decreases (tensile force increases) as λ (or μ) decreases.

2.3. Flatness of Contact Area

It should be noted that during the above derivation, the surface energy of contact area, $U_S = -2\gamma\pi a^2$, was used. Again, it is emphasized that γ is defined as the surface energy per unit area of a surface [6]. So it is not difficult to conclude from this surface energy expression that the contact area of πa^2 is flat. Also, this contact area of πa^2 is a geometric area and the roughness effect is not considered here. To have the adhesion contact area equal to the geometric area, the surfaces of both contacting bodies must be 'molecularly smooth' [22]. In reality, the adhesion contact area is not equal to the geometric area because of roughness. Recently, the breakdown of continuum model for mechanical contact on a nanometer scale due to the effect

Downloaded by [Institute of Mechanics] at 02:37 31 October 2013

of roughness was discussed [23]. This flatness property of contact area for sure has an influence on the P–a curves. Before discussing it, an elasticity proof for that the contact area of the Hertz and JKR models is flat is first presented.

The gap ($D(r)$) between two contacting bodies is expressed as [15, 19, 24, 25]

$$D(r) = -\delta + z_0 + \frac{r^2}{2R} + u(r), \tag{20}$$

where z_0 arises in equation (20) when the surface force is due to the Lennard-Jones (L-J) potential. When the surface force is due to the L-J potential, the two 'contacting' bodies must separate with a certain distance because the surface force induced by the L-J potential becomes singular when the separation is zero. In the JKR model and the 'soft' contact model of Hughes and White [26], there is no such interatomic separation z_0 term. Here $u(r) = u_1(r) + u_2(r)$ and $u_1(r)$, $u_2(r)$ are the elastic deformations inside the contact area of two contacting bodies. In the JKR model, $u(r)$ is the elastic deformation due to the contact pressure $p(r)$. In the numerical computation which assumes no contact pressure profile, $u(r)$ is induced by the surface force due to the L-J potential [15, 19, 24, 25]. As indicated in equation (2), $p(r)$ consists of two terms: the Hertzian pressure $p_0(1 - r^2/a^2)^{1/2}$; and $p_0'(1 - r^2/a^2)^{-1/2}$, which is often referred to as the Boussinesq pressure [19]. The elastic deformation due to the Hertzian pressure is $u_{\mathrm{H}}(r) = \delta - \frac{r^2}{2R}$ [8] and the elastic deformation due to the Boussinesq pressure is a constant $u_{\mathrm{B}}(r) = D_0$ (D_0 is a constant) [8, 19]. As linear elasticity applies, $u(r)$ is obtained by superposing u_{H} and u_{B} as follows

$$u(r) = u_{\mathrm{H}} + u_{\mathrm{B}} = \delta - \frac{r^2}{2R} + D_0. \tag{21}$$

By substituting equation (21) into equation (20) and δ, $r^2/(2R)$ terms are canceled out. The gap distance in the contact area is then derived as a constant $D(r) = z_0 + D_0$, which physically means the flatness of contact area. So it is the JKR contact pressure $p(r)$ of equation (2) which results in the flatness of contact area. As the Boussinesq pressure contributes only a constant elastic deformation ($u_{\mathrm{B}}(r) = D_0$), the contact area due to the Hertz pressure is also flat.

If the surface interaction inside the contact area is treated as the (vdW) force due to L-J potential and when $r < r_0$, as shown in Fig. 5 the separation of two surfaces is less than z_0 and the repulsive vdW force pushes the elastic bodies, so the contact pressure is compressive. When $r_0 \leqslant r \leqslant a$, the separation is larger than z_0, the attractive vdW force pulls the elastic bodies and the contact pressure becomes tensile. The schematic of Fig. 5 was originally given by Tabor [22]. From this viewpoint of vdW force, the contact surface of the JKR model cannot be exactly flat because it is the curviness of the contact surface causing the compressive–tensile contact pressure profile in the JKR model, which is also reflected in Fig. 4(a). In general z_0 is very small compared with a and the flatness is thus a good approximation, except for few contact scenarios as analyzed below. As shown in the numerical results of

Downloaded by [Institute of Mechanics] at 02:37 31 October 2013

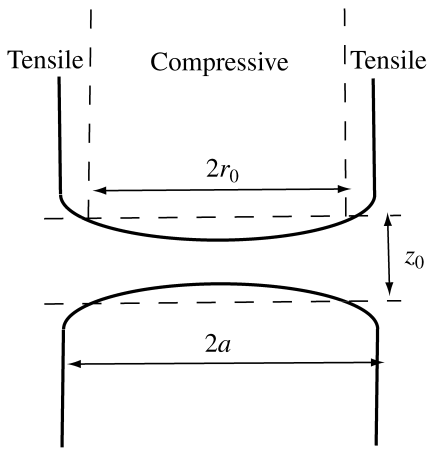

Figure 5. The JKR contact pressure and contact surface profiles.

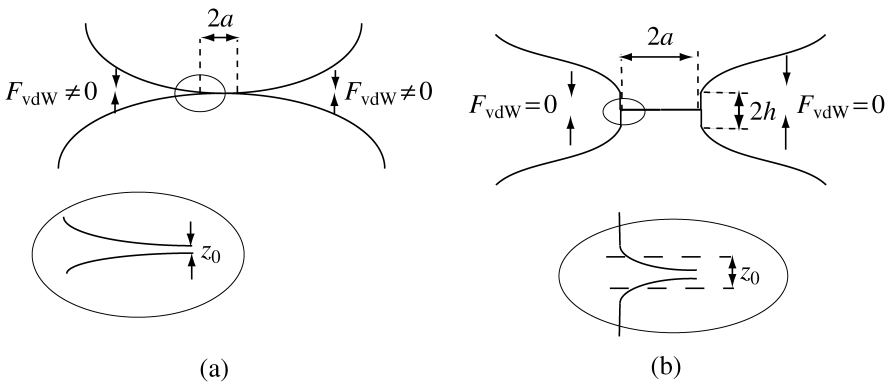

Figure 6. The contact scenarios of the DMT (a) and JKR models (b).

Feng [24, 25], for very small Tabor number cases (see Fig. 5(a) in reference [24] and Fig. 6(a) in reference [25] or relatively large negative δ case with relatively large Tabor number ($\mu = 3$) (see Fig. 8(a) in reference [24]), the contact area is obviously not flat, though the deviation from the flatness around the contact edges is relatively small. Similar numerical results are also shown by Attard and Parker [27] that the flatness is a good approximation for the contact profile due to the surface force of the L-J potential though a closer look reveals that it is not exactly flat (see Fig. 6(a) and 6(b)). It is also noticed that as shown by Attard and Parker [27], the surface profile just before 'jumping on' to contact is very curvy and the contact surface profile due to exponentially decaying repulsive surface force (not the L-J type surface force) is also very curvy. For the Bradley model of rigid spheres, the flatness of contact area is not permitted [17]. In equation (20) the parabolic term of $r^2/2R$ is used to approximate the (undeformed) sphere profile. Without this approximation, the result $D(r) = z_0 + D_0$ cannot be obtained. Maugis [28] uses the exact profile

Downloaded by [Institute of Mechanics] at 02:37 31 October 2013

of sphere rather than the parabolic approximation to derive the contact of elastic spheres and significant solution deviation from that of the JKR model for certain scenarios is shown. However, for the Hertz model or the JKR model to apply, the following conditions must be satisfied: the dimension of contact area must be small compared (a) with the dimensions of each contacting body and (b) with the relative radii of curvatures of the surfaces [8]. Only when these two conditions are satisfied, linear elasticity (linear elastic fracture mechanics) and half-space solution used in the derivation of the Hertz and JKR models can be applied. The two (constraint) conditions above guarantee the accuracy of the parabolic approximation.

Hughes and White [26] developed the model for the 'soft' contact. The word 'soft' is used to differentiate it from the 'hard' contact model. In the 'soft' contact theory, the key concept of perfect flatness over a well-defined contact area in the 'hard' contact theories is replaced by the physically consistent surface force [26]. This 'soft' contact approach was later used by Argento *et al.* [29], Attard and Parker [27], Feng [24, 25], Greenwood [15], Muller, Yushchenko, Derjaguin [19, 30] and Wu [31]. When extending the JKR model or the Hertz model to the problem of an elastic sphere indenting a cavity [32] or the contact problem of a soft body with a hard body, the effect of curved contact surface should be considered. As shown in both the experiment and analysis of Goodman and Keer [32], their contact radius is significantly smaller than that predicted by the Hertz model. Also shown in the experiments involving a highly compliant substrate in contact with rigid particles by Rimai *et al.* [33], their measured contact radius data deviate significantly from those predicted by the JKR model. Here it needs to be emphasized that the JKR model was established for two similar homogeneous solids in contact [34], not for the rigid-soft contact scenario.

3. Surface Interaction Outside the Contact Area: Equilibrium Analysis

3.1. Transitions Between the Hertz, JKR, MD, DMT and Bradley Models

Equation (11) is the key to understand the transitions between the Hertz, JKR, MD, DMT and Bradley models. It should also be pointed out that there are two contact scenarios as shown in Fig. 6. For the DMT contact scenario in Fig. 6, the surface interaction outside the contact area is significant. Therefore, the DMT model considers the influence of surface interaction (vdW force) due to the Lennard-Jones potential outside the contact area. While, the JKR model assumes that there is a 'neck' formation around the contact zone (see Fig. 6). If the neck height h is large compared with z_0, the surface interaction outside the contact area can be ignored because the Lennard-Jones potential induced surface interaction decays rapidly with the increase of the separation distance [6, 15, 19]. The 'neck' height is the key to differentiate the DMT and JKR models. Tabor [22] introduced a dimensionless number μ now known as the Tabor number for this differentiation. Physically, the Tabor number is the ratio of (the order of) neck height to z_0. For a large Tabor number, the materials outside the contact area are well separated; therefore, the surface

Downloaded by [Institute of Mechanics] at 02:37 31 October 2013

Downloaded by [Institute of Mechanics] at 02:37 31 October 2013

interaction is very small and can be ignored, which is the JKR contact scenario. For a small Tabor number, the surface interaction outside the contact area is significant; therefore, it corresponds to the DMT contact scenario. The DMT model uses the Hertzian contact pressure profile, which in essence as pointed by Tabor [22] has the main drawback of neglecting the deformation due to the surface interaction close to the contact edge. This surface interaction around the contact edges is also responsible for the tensile contact pressure and the singularity in the JKR contact pressure at the edges [7, 8]. Tabor [22] argues that for the DMT model to consider the surface interaction outside the contact zone, the large attractive forces around the contact edge will pull some extra regions into contact (this is also why in Fig. 1 the JKR contact radius is always larger than DMT's before the jumping separation) and form a 'neck'. Otherwise, more and more regions will be pulled into contact without an arrest mechanism. As seen in the JKR contact scenario of Fig. 6, the 'neck' formation separates the edges of contacting bodies, which reduces the surface interaction outside the contact area. Therefore, the 'neck' formation is an arrest mechanism to prevent more regions around edges to be pulled into contact by the large attractive forces of surface interaction. Tabor's experimental observation also supports the neck-forming JKR contact scenario. The Tabor number plays an important role in differentiating different models and defining their application ranges [16].

Equation (11) is an equilibrium equation, which indicates that the external force is equal to the internal force. Here it is emphasized that P is defined as the external loading force. P is the control parameter. While, the external load should also include the force F_{vdW} due to the interaction between two surfaces outside the contact area as shown in Fig. 6. F_{vdW} is not the control parameter. The internal force $\int_0^a 2\pi r p(r)\,\mathrm{d}r$ is due to the elastic deformation. The surface interaction inside the contact area is accounted as the internal force and it determines p_0' as shown in equation (10). Equation (11) now should be rewritten as follows

$$P_{\mathrm{external}} = P + F_{\mathrm{vdW}} = \left(\frac{2}{3}p_0 + 2p_0'\right)\pi a^2. \tag{22}$$

For the expression for F_{vdW}, there are several approximations [5, 15, 19, 30]. A more general and precise way of numerically calculating F_{vdW} is given by Argento *et al.* [29]. Here the *Derjaguin approximation* [5, 6] is used, which states

$$F_{\mathrm{vdW}} = 2\pi R W(D). \tag{23}$$

Where $W(D)$ is the interaction energy of two spheres with a separation gap of D [6]. $W(D)$ for different geometries is given in Israelachvili's book [6] and $W(z_0) = 2\gamma$ for two spheres.

For the Bradley model, p_0 and p_0' are zero because of no elastic deformation of rigid spheres. From equations (22) and (23) and at $D = z_0$, the Bradley pull-off force is $P = -F_{\mathrm{vdW}} = -4\pi R\gamma$. For varying D, $P = -F_{\mathrm{vdW}} = -2\pi R W(D)$, which is often referred to as the Bradley model though Bradley [4] actually only calculated $D = z_0$ case and it was Derjaguin [5] who calculated the varying D case [15]. For the Hertz model, it is purely an elastic deformation problem and

Downloaded by [Institute of Mechanics] at 02:37 31 October 2013

there is no adhesion effect. Therefore, F_{vdW} is zero and adhesion-induced p_0' is also zero. Equation (22) now becomes $P = (2/3)\pi p_0 a^2$ and with p_0 definition of equation (3), the Hertz P–a relation of $P = 4Ea^3/(3R)$ is derived. For the DMT model, $F_{\mathrm{vdW}} = 4\pi R\gamma$. The DMT model also assumes Hertzian contact pressure profile, so $p_0' = 0$. Therefore, from equations (22), (23) and (3), the DMT P–a relation is derived as $P = -4\pi R\gamma + 4Ea^3/(3R)$. Compared with the Hertz P–a curve, the DMT P–a curve is simply a $4\pi R\gamma$ shift from Hertzian. This fact was first recognized by Maugis [3]. For the JKR model, $F_{\mathrm{vdW}} = 0$. By using the definitions of p_0 in equation (3) and p_0' in equation (10), the JKR P–a curve of equation (1) is also derived from equation (22). As shown by Maugis [3] and also in Fig. 1, for the MD model, $-4\pi R\gamma \leqslant F_{\mathrm{vdW}}^{\mathrm{MD}} \leqslant 0$, which in essence modifies the Derjaguin approximation for the surface/vdW force outside the contact area. Here we also need to point out the following facts that to use $-4\pi R\gamma$ in the DMT model to account for the surface/vdW force outside the contact area is problematic when the contact radius a is relatively large. This Derjaguin approximation of $-4\pi R\gamma$ is for the surface attraction of two spheres separated with a distance of z_0 and curvy spheroid surface profiles. However, the DMT model assumes Hertzian contact pressure and the contact area is thus flat as analyzed above. So here the flatness of contact area due to the Hertzian contact pressure and the Derjaguin approximation of assuming curvy spheroid surfaces is inconsistent. When a is relatively large, the flat contact area due to the Hertzian pressure is also relatively large, which makes the Derjaguin approximation inaccurate. Therefore, in the DMT model the Derjaguin approximation which is independent of contact radius a is not a good approximation when a is relatively large.

Equation (22) is non-dimensionalized as follows using equations (3) and (10)

$$(F - A^3)^2 = 4A^3 + \frac{16}{3}\kappa + \frac{16}{9}\kappa^2. \tag{24}$$

The dimensionless number κ is defined as $\kappa = W(D)/(2\gamma)$. When $\kappa = 0$ equation (24) recovers the JKR model of equation (13). In equation (24), $4A^3 + \frac{16}{3}\kappa$ is due to the Boussinesq pressure p_0'. If only the Hertzian contact pressure exists, equation (24) becomes:

$$F = A^3 - \frac{4}{3}\kappa. \tag{25}$$

Equation (25) is the Hertz model when $\kappa = 0$ and the DMT model when $\kappa = 1$. In the DMT contact scenario, $\kappa = 1$ when the Derjaguin approximation is applied; at the same time μ is also very small because of the no/small 'neck' formation. In the JKR contact scenario, $\kappa = 0$ because the 'neck' height is very large compared with z_0 and the surface interaction outside the contact area can thus be ignored; μ approaches infinity due to the same reason, i.e., the 'neck' height is very large compared with z_0. The Tabor number μ is the ratio of neck height to the inter-atomic equilibrium separation z_0. A larger Tabor number means a larger neck height (z_0 is fixed), which results in larger gap distance and thus in smaller

F_{vdW} and $W(D)$. Therefore, κ and μ are related as $\kappa \propto \mu^{-n}$ (n is a positive number depending on the geometries and force due to the Lennard-Jones potential of two contacting elastic bodies).

3.2. Discussion on the Definitions of Contact Radius

It is noticed that when the Derjaguin approximation is considered, F_{vdW} is independent of a. In the Bradley model of $P = -2\pi RW(D)$, contact radius a does not appear. The rigid spheres of the Bradley model are not allowed to deform and the two spheres are explicitly separated with a distance of D. Therefore, a natural question arises: what is the contact radius/area in the Bradley model? For those carrying out numerical computation on the contact of elastically deformable spheres under the L-J potential influence, they also face the problem and difficulty of defining contact radius [15, 25, 27]. If the flattened area is defined as the contact area (then the spheres in the Bradley model are not in 'contact'), as argued by Attard and Parker [27], there is actually no exactly flat area in the 'contact area' if a closer look is taken. Attard and Parker's attitude on the definition of contact area is a little bit radical as reflected in their statement that "any definition of the contact radius is somewhat arbitrary" [27]. Greenwood [15] proposed that the edge of the contact area is the point where the tensile pressure reaches the maximum. However, Feng [25] argues that Greenwood's definition is not consistent with that of traditional contact mechanics where the contact area is usually taken as the area with compressive pressure. Feng's conclusion is that any rigorous definition of 'contact area' can be disputable when considering the L-J potential influence [25]. So, instead of arguing the definition of contact area, Greenwood [15], Feng [24, 25], and Attard and Parker [27] plotted P–δ curves instead of P–a curves. Although experimentally measuring the normal displacement δ is much easier than measuring the contact radius a [35], the P–a curves are presented in many theoretical analyses [1, 3, 7–9, 32] and experiments [7, 32, 33, 36, 37]. This paper adopts the P–a curves for comparison reasons. The conversion of P–a curves into P–δ curves is available in Maugis' paper [3]. For the Hertz model with the contact pressure of $p_0(1 - r^2/a^2)^{1/2}$, the contact radius is the point ($r = a$) where the (compressive) pressure disappears; for the JKR model with the contact pressure of $p_0(1 - r^2/a^2)^{1/2} + p_0'(1 - r^2/a^2)^{-1/2}$, the contact radius is the point where the (tensile) pressure becomes singular. Therefore, as pointed out by Feng [25], these two definitions of contact radius are different, which also contributes to the difference in the JKR and Hertz models besides the physical reasons (the contact pressure profiles and the surface interaction). For the MD model with the contact pressure of $p_0(1 - r^2/a^2)^{1/2} + p_{\mathrm{d}}(r)$, the contact radius is defined as the one at which the separation distance of two contacting surfaces reaches $z_0 + h_0$.

4. Conclusion

Surface interactions both inside and outside the contact area are the key to understand the transitions between the different models. The surface interaction inside

Downloaded by [Institute of Mechanics] at 02:37 31 October 2013

the contact area together with the elastic deformation determines the contact pressure profiles and different contact models assume/have different pressure profiles. The surface interaction outside the contact area together with the external mechanical loading determines the total external load, which, in turn, affects the system equilibrium. The 'neck' formation and different approximations for the surface interaction outside the contact area result in different expressions for the equation of equilibrium. Different models have different contact pressure profiles and as a result their definitions of the contact radius have different physical meanings. The definition difference together with the modeling differences on how to evaluate the surface interactions inside and outside the contact area contributes to the difference in P–a curves obtained by different contact models. Because some of contact pressure profiles mathematically lead to the conclusion of flat contact area, one should be cautious in the application of certain contact models for those scenarios that may have curvy contacting surfaces.

Acknowledgements

This work was supported by the National Natural Science Foundation of China (NSFC, Grant Nos 10502050 and 10721202).

References

1. H. Hertz, *Miscellaneous Papers*. Macmillan, London, UK (1896).
2. J. Boussinesq, *Compt. Rend. Acad. Sci.* **XCVI**, 245 (1883).
3. D. Maugis, *J. Colloid Interface Sci.* **150**, 243 (1992).
4. R. S. Bradley, *Phil. Mag.* **13**, 853 (1932).
5. B. V. Derjaguin, *Kolloid. Zh.* **69**, 155 (1934).
6. J. N. Israelachvili, *Intermolecular and Surface Forces*. Academic Press, London, UK (1985).
7. K. L. Johnson, K. Kendall and A. D. Roberts, *Proc. Roy. Soc. London A* **324**, 301 (1971).
8. K. L. Johnson, *Contact Mechanics*. Cambridge University Press, Cambridge, UK (1985).
9. B. V. Derjaguin, V. M. Muller and Yu. P. Toporov, *J. Colloid Interface Sci.* **53**, 314 (1975).
10. B. V. Derjaguin, V. M. Muller and Yu. P. Toporov, *J. Colloid Interface Sci.* **67**, 378 (1978).
11. D. Tabor, *J. Colloid Interface Sci.* **67**, 380 (1975).
12. B. V. Derjaguin, V. M. Muller and Yu. P. Toporov, *J. Colloid Interface Sci.* **73**, 293 (1979).
13. D. Tabor, *J. Colloid Interface Sci.* **73**, 294 (1979).
14. D. S. Dugdale, *J. Mech. Phys. Solids* **8**, 100 (1960).
15. J. A. Greenwood, *Proc. Roy. Soc. London A* **453**, 1277 (1997).
16. K. L. Johnson and J. A. Greenwood, *J. Colloid Interface Sci.* **192**, 326 (1997).
17. K. S. Kim, R. M. McMeeking, K. L. Johnson, *J. Mech. Phys. Solids* **46**, 243 (1998).
18. A. A. Griffith, *Phil. Trans. R. Soc. London A* **221**, 163 (1920).
19. V. M. Muller, V. S. Yushchenko and B. V. Derjaguin, *Colloids Surfaces.* **7**, 251 (1983).
20. G. I. Barenblatt, *Adv. Appl. Mech.* **7**, 55 (1962).
21. E. Barthel, *J. Colloid Interface Sci.* **200**, 7 (1998).
22. D. Tabor, *J. Colloid Interface Sci.* **58**, 2 (1977).
23. B. Luan and M. O. Robbins, *Nature* **435**, 929 (2005).

Downloaded by [Institute of Mechanics] at 02:37 31 October 2013

24. J. Q. Feng, *Colloids Surfaces. A* **172**, 175 (2000).
25. J. Q. Feng, *J. Colloid Interface Sci.* **238**, 318 (2001).
26. B. D. Hughes and L. R. White, *Quart. J. Mech. Appl. Math.* **32**, 445 (1979).
27. P. Attard and J. L. Parker, *Phys. Rev. A* **46**, 7959 (1992).
28. D. Maugis, *Langmuir* **11**, 679 (1995).
29. C. Argento, A. Jagota and W. C. Carter, *J. Mech. Phys. Solids* **45**, 1161 (1997).
30. V. M. Muller, V. S. Yushchenko and B. V. Derjaguin, *J. Colloid Interface Sci.* **77**, 96 (1980).
31. J. J. Wu, *Int. J. Solids Structures* **43**, 1624 (2006).
32. L. E. Goodman and L. M. Keer, *Int. J. Solids Structures* **1**, 407 (1965).
33. D. S. Rimai, L. P. DeMejo and W. B. Vreeland, *Langmuir* **10**, 4361 (1994).
34. K. L. Johnson, *Langmuir* **12**, 4510 (1996).
35. F. Q. Yang, X. Z. Zhang and J. C. M. Li, *Langmuir* **17**, 716 (2001).
36. R. G. Horn, J. N. Israelachvili and F. Pribac, *J. Colloid Interface Sci.* **115**, 480 (1987).
37. J. N. Israelachvili, E. Perez and R. K. J. Tandon, *J. Colloid Interface Sci.* **78**, 260 (1980).

Downloaded by [Institute of Mechanics] at 02:37 31 October 2013